Engineering Structures 188 (2019) 233–248

Contents lists available at ScienceDirect

Engineering Structures

journal homepage: www.elsevier.com/locate/engstruct

Tile vaults as integrated formwork for reinforced concrete: Construction, experimental testing and a method for the design and analysis of two-dimensional structures

David López López[a,*], Pere Roca[b], Andrew Liew[c], Tom Van Mele[c], Philippe Block[c]

[a] ETH Zurich, Institute of Technology in Architecture, Block Research Group Stefano-Franscini-Platz 1, HIB E45, 8093 Zurich, Switzerland
[b] Universitat Politècnica de Catalunya, Department of Civil and Environmental Engineering, Spain
[c] ETH Zurich, Institute of Technology in Architecture, Block Research Group, Switzerland

ARTICLE INFO

Keywords:
Catalan vault
Guastavino vault
Tile vault
Masonry
Reinforced brick
Formwork
Concrete shell
Limit analysis
ELARM

ABSTRACT

Tile vaults are traditional, unreinforced masonry structures made of thin bricks (tiles), mortar and fast-setting cement or gypsum. They can be constructed without the need for a formwork, except at the boundaries, making them inherently economic. Tile vaults have historically provided a solution for the efficient construction of vaulted structures. Today, they can be used as permanent formwork for concrete shells, allowing for a significant reduction of the construction cost and waste produced, due to the possibility of reducing or even eliminating the need for traditional formwork. The concrete can be poured directly onto a tile-vaulted formwork to form a composite structure.

This paper presents a technique for the construction of single-curvature shells consisting of a composite structure combining tile vaulting and reinforced concrete. A method for the design of these composite vaults and the assessment of their strength and stability against external loading is also presented. This method is based on limit analysis but takes into account the reinforcement's contribution to the composite cross-section's bending capacity.

The equilibrium method is implemented computationally to provide fast results for the user. It provides graphical and intuitive results and opens the possibility for the future extension to fully three-dimensional problems. The design and structural analysis method is called Extended Limit Analysis for Reinforced Masonry (ELARM).

Both the proposed construction technique and the computational method have been validated through experimental research. The feasibility of the building technique has been validated by the construction of two full-scale prototypes. In addition, the prototypes have been load-tested to failure to compare the results with those predicted by ELARM.

1. Introduction

Tile vaults (sometimes also referred to as thin-tile, timbrel, Catalan or Guastavino vaults) are masonry structures made with thin bricks (tiles), mortar and fast-setting cement or gypsum. The bricks are placed flat, building up to two, three or more courses. Traditionally, tiles are used because of their light weight, which is a necessary condition to build the first course "in space" without supporting falsework (Fig. 1). The first course is achieved using the quick adhesion of fast-setting cement or gypsum. The bricks bind within seconds to the edge walls, or the already finished arches/stable sections, eliminating the need for centring [1]. Using this first layer as a stay-in-place formwork, the second and subsequent courses can be set with lime or Portland cement mortar. The ability of the courses to be built without support and in stable sections, is one of the most relevant characteristics of this technique and what makes it inherently economic. Tile vaulting is currently being rediscovered in contemporary architecture and has been used in a series of recent projects that investigate novel applications and design possibilities of the traditional technique [2–9].

Concrete shell construction was particularly popular from the 1920s to the early 1960s. A main reason for concrete shell's demise after this period can be found in the construction costs [11], specifically the cost of the formwork, which is typically expensive, complex and wasteful. Using tile vaults as stay-in-place formwork for concrete shells could

* Corresponding author.
E-mail address: lopez@arch.ethz.ch (D. López López).

https://doi.org/10.1016/j.engstruct.2019.03.034
Received 15 June 2018; Received in revised form 6 March 2019; Accepted 12 March 2019

Fig. 1. Construction "in space" of a tile-vaulted stair [10].

significantly reduce construction costs and material waste, making concrete shells more economic and sustainable for modern construction. The construction costs are reduced mainly due to the low cost of the materials involved, and to the fact that no additional formwork or related foundations are needed. The use of the tile vault as formwork does not cause a large increase of the total thickness of the shell because the tile vault is structural and contributes by resisting, at least, the overall self-weight of the composite system. As an additional bonus, the use of a tile vault as a permanent formwork has the added value of the architectural quality: if left exposed, it adds a unique, unconventional finish. Compared to unreinforced masonry structures, the addition of reinforcement allows a minimum thickness for long-span shells, which might become too large and heavy otherwise, and allows for the construction of expressive structures beyond compression-only designs, capable of resisting tensile stresses and bending moments. Note, however, that non-compression-only structures need a formwork for their construction in the areas of the structure where the tile vault does not work only in compression under its self-weight.

The combination of masonry and reinforced concrete creates a new type of composite structure that needs new calculation methods and models to deal with the specific features of the system. There is currently no method for designing these structures and no (simple) model to analyse and assess them. This paper therefore presents a simple and user-friendly method for the design and structural analysis of singly-curved, reinforced tile vaults. The method is called Extended Limit Analysis for Reinforced Masonry (ELARM) and is an extension of the work by Roca et al. [12] on the assessment of the structural behaviour of the mentioned composite structure. ELARM applies limit analysis [13–15] as is common with regular masonry, but using the boundaries of a vault whose thickness is virtually increased to indirectly take into account the additional tensile and bending strength provided by the steel reinforcement. This method benefits from the simplicity of limit analysis to safely design and assess the strength and stability of singly-curved, concrete-reinforced, tile-vaulted structures against self-weight and external loading. Moreover, the design method allows for the assessment of the structure during all of the construction stages, as it can be also utilized to verify the stability of the tile vault subject to both its self-weight (the tile vault in isolation) and the weight of the concrete layer prior to its hardening where it is acting as dead weight. ELARM has been parametrised and implemented computationally, resulting in a fast, straightforward and user-friendly tool that provides graphical and intuitive results.

The proposed construction technique required physical tests to validate both the feasibility of construction technology and the performance of the numerical method. This validation has been attained by constructing and testing two full-scale prototypes in the laboratory. Specifically, the numerical method has been validated by comparing its predictions, in terms of the collapse mechanism and ultimate loads, with the experimental results.

This paper presents a construction system using the tile vault as integrated formwork for reinforced concrete, a method for the design and analysis of two-dimensional arched structures built with this technique, experimental research to validate both of them and applications of the method including form-finding and optimisation procedures. The construction system is explained in Section 2, whereas Section 3 focuses on the design and structural analysis method, followed by its computational implementation in Section 4. The experimental research is described in Sections 5 and 6, presenting load tests on full-scale prototypes and material characterisation, respectively. The results of the experimental research and those provided by the method are compared in Section 7. The last section before the conclusions is Section 8, which presents examples of different applications of the method.

2. Construction system

The proposed structure is composed of a tile vault and an added

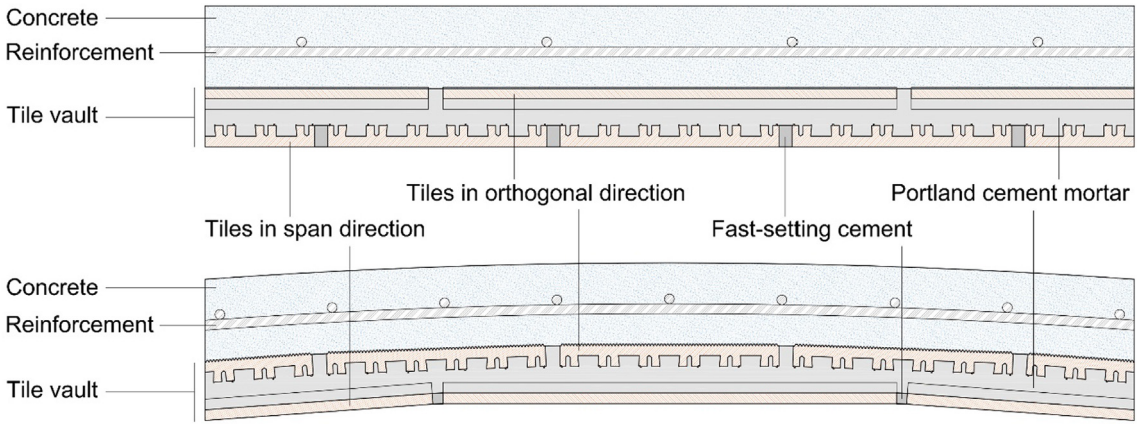

Fig. 2. Possible transversal and longitudinal cross-sections of the composite system. Featuring a two-layered tile vault and reinforced concrete.

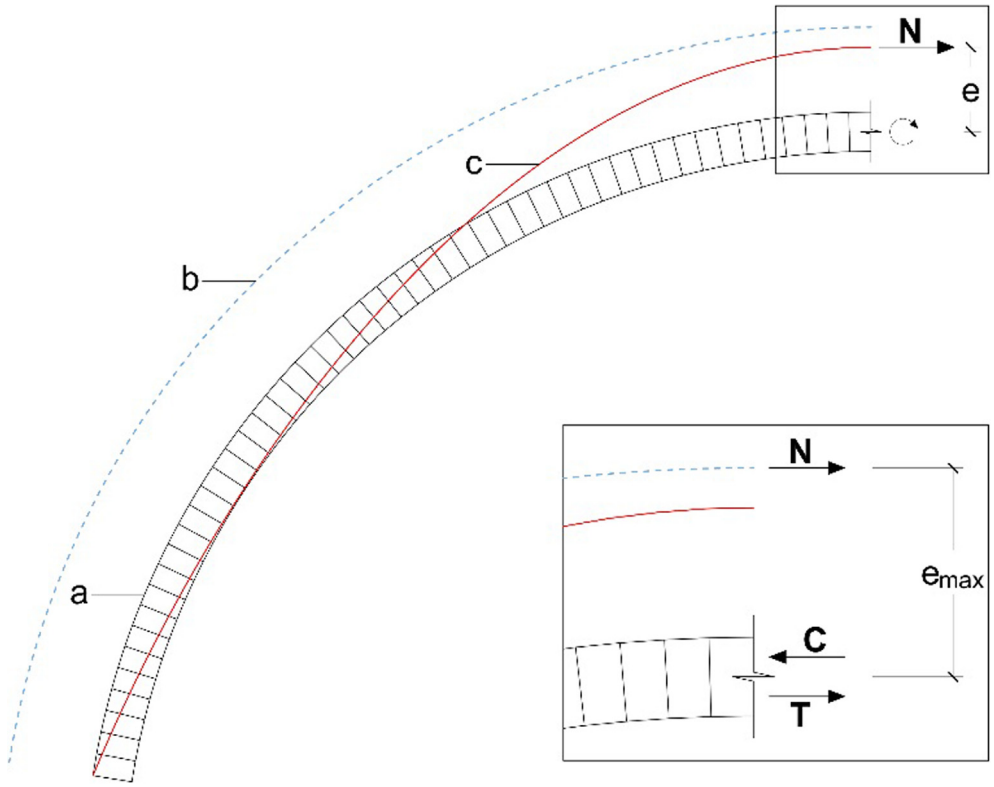

Fig. 3. Thrust line located outside of the vault's thickness creating a bending moment; (a) reinforced masonry arch, (b) upper virtual thickness, and (c) thrust line. (Lower right) schematic distribution of forces for the ultimate positive bending moment.

layer of reinforced concrete working together as a composite system (Fig. 2). The tile vault acts as permanent formwork for the concrete during its hardening, supporting the concrete's weight and construction loads. After the concrete hardening, the structure becomes a composite system.

The first course of tiles is laid with fast-setting cement or gypsum. For the second and subsequent courses, and also for the mortar beds between them, regular lime or Portland cement mortar is used. Continuous joints between courses through the thickness of the masonry should be avoided, as they create weak points in the structure.

A longer spanning structure will require a thicker tile vault to be able to support the self-weight of the structure and the construction loads. In order to achieve a specified thickness, the tile vault can, if needed, be built with bricks of different thicknesses. To keep a light first layer of bricks, necessary for building without formwork, hollow bricks instead of solid tiles can be used. Furthermore, the second and subsequent courses can be built with heavier and thicker bricks to build up structural depth more effectively, as they are not built "in space". Striped or rough bricks can provide the required bond between tile vault and concrete to guarantee the composite behaviour of the hybrid system. If this interface bond is not sufficient, shear connectors can also be used.

The proportioning of the concrete mixture plays an important role to achieve a good balance between low flowability and a certain degree of self-compaction, which are material requirements that will ease the construction process. Low flowability is necessary to work on steep surfaces with a certain degree of self-compaction to avoid the need for intense vibration on the masonry structure. Reinforcement also offers many possibilities depending on the structure's features. Reinforcement bars (rebars) can be placed easily on singly-curved or ruled surfaces, but fibre or mesh/textile reinforced concrete may be a better choice for free-form structures which otherwise would require complex reinforcement plans and a difficult pre-bending process of the bars. In addition, non-metallic reinforcement may reduce the overall thickness of the shell as the otherwise-mandatory concrete covering to prevent corrosion is not required.

3. Extended limit analysis of reinforced masonry

3.1. Background

Jacques Heyman set down in 1966 the modern formulation of limit analysis for masonry arches [14]. Three assumptions were a key aspect in his theory: (1) masonry has no tensile strength, (2) the compressive strength of masonry is effectively infinite, and (3) sliding of one masonry unit upon another cannot occur. The great success of Heyman's assessment framework relies on the simplicity of the method and its application to many types of masonry structures. These foundations eliminated doubts expressed 13 years before by Kooharian, on the discussion of his article from 1952 "*Limit Analysis of Voussoir (Segmental) and Concrete Arches*" [13,16]. These doubts were based on his own research and were supported by the comprehensive theoretical and experimental research by Alfred J. S. Pippard [17–19]. Kooharian mainly expressed the need to consider the influence of the mortar's tensile capacity and the limited compressive strength of the material (which may cause crushing failure) in the analysis of unreinforced masonry structures. About the sliding of masonry units, he quoted Pippard and Chitty: "*Slip only occurred in the tests as an accompaniment of crushing or spalling, and never as a distinct type of failure*" [19]. In the discussion part of Kooharian's article [16], he also mentioned the suitability of the theory of limit analysis "*to structures made of such plastic materials as reinforced concrete*". Limit analysis is framed within the plastic theory and its applicability is therefore restricted to structures able to develop the sufficient number of hinges to become a ductile mechanism. Further references support the suitability of limit analysis for the kind of structures presented in this document; it was also proposed as a tool for the analysis of reinforced concrete arches by Lourenço et al. [20], reinforced masonry by Roca et al. [12] and

unreinforced masonry including tensile capacity by Ramaglia et al. [21] and Fabbrocino et al. [22].

The method presented in this paper is based on limit analysis, but takes into account the finite compressive strength of the tile vault and concrete as well as the tensile capacity of the reinforcement embedded within the concrete. It allows both design and structural analysis and introduces the possibility to include an additional material, being suitable for the proposed composite construction system.

3.2. Concept

The presented method analyses the composite cross-section to obtain its ultimate positive and negative moment for the given axial load, which varies along the structure and is determined by the self-weight and the external loads. The ratio between the ultimate moment and the axial force is equal to the maximum possible eccentricity (Fig. 3). The eccentricity related to the positive moment defines the upper limit of the new virtual thickness and the eccentricity related to the negative moment defines the corresponding lower limit. As is done in the classical theory of limit analysis of masonry arches, the structure is divided in a number of virtual voussoirs, which allow the construction of the thrust line and sets the specific sections where axial forces, moments and eccentricities are calculated.

The thrust line and axial forces can be obtained graphically or analytically. The stability of the vault is verified when it is possible to find a thrust line, in equilibrium with the applied loads, that is fully contained within the new virtual thickness of the vault, meaning that the safe theorem is satisfied. The uniqueness theorem can also be applied to obtain the collapse load and mechanism of the composite vault.

The support conditions of the vault are of great importance for the definition of the thrust line and the stability of the vault. If the vault is pinned at its supports (Fig. 4k) with a single contact point, then the thrust line must pass through that point. In the case of a support consisting of a contact surface, unable to take bending moments, the thrust line can pass through any point of the mentioned surface. Finally, in the case of a fixed support (Fig. 4a), the limits for the thrust line at the supports coincide with the virtual thickness.

ELARM is not only limited to the design and structural analysis of composite vaults with a cross-section as given in Fig. 2. This method is applicable for reinforced concrete, reinforced masonry and reinforced composite (masonry and concrete) arched structures, provided that the failure mode corresponds to that of a ductile mechanism characterised by the development of a sufficient number of hinges. Additionally, for concrete-reinforced tile-vaulted structures and prior to the hardening of the concrete, the method presented can be also utilized to verify the possibility of finding an admissible thrust line solution for the tile vault subject to its self-weight and the tile vault subject to its self-weight and the addition of the dead weight of the concrete layer.

3.3. Geometry

The geometry of the vault is defined by its intrados, i.e. its inner surface, and the thicknesses of the tile vault and the concrete layer, h_{tv} and h_c. The vault is divided into a number of fictitious voussoirs, with a tile vault voussoir and a concrete voussoir in each transversal cross-section. The voussoirs' volumes of these materials need to be considered separately to compute their weights, as the tile vault and the concrete have different specific weight values.

3.4. Loads

External, vertical and horizontal loads (VL_i and HL_i) can be applied at any extrados (outer surface) voussoir edge (Fig. 5). Furthermore, horizontal loads (Hw_{tv_i} and Hw_{c_i}) can be applied at the centroid of every tile vault and concrete portion (Gv_{tv} and Gv_c) within each voussoir. These forces are calculated as the self-weight of the voussoir (W_{tv_i} and W_{c_i}), multiplied by a factor specified by the user. This feature allows for a quick and preliminary equivalent-static seismic analysis by applying horizontal loads as a multiplier of the gravitational loads.

3.5. Thrust line

ELARM determines the thrust line analytically. When using limit analysis for the study of an arch, different thrust lines that are in equilibrium with the applied loads, can be obtained by setting different values to three independent variables defining their geometry. In the presented method, these three variables are (highlighted in blue in Fig. 5): (1) the horizontal thrust at the left support, H_l, (2) the end point of the thrust line at the left support, e_l, defined by its distance from the intrados, and (3) the end point of the thrust line at the right support, e_r, also defined by its distance from the intrados. The forces acting on the global structure and those acting on an individual virtual voussoir are indicated in Fig. 5.

The global equilibrium of the vertical forces, horizontal forces and moments can be expressed with the following equations, respectively:

$$V_l + V_r = W_c + W_{tv} + \sum_{i=1}^{n} VL_i \tag{1}$$

$$H_r = Hw_c + Hw_{tv} + \sum_{i=1}^{n} HL_i + H_l \tag{2}$$

$$H_l y_{H_l} + \sum_{i=0}^{n} HL_i y_{HL_i} + \sum_{i=0}^{n} VL_i x_{VL_i} + W_c x_{W_c} + Hw_c y_{Hw_c} + W_{tv} x_{W_{tv}} + Hw_{tv} y_{Hw_{tv}} = V_l x_{V_l} + H_r y_{H_r} + V_r x_{V_r} \tag{3}$$

where n is the number of fictitious voussoirs, i indicates the specific voussoir on which the force, VL_i or HL_i, is applied and x_o and y_o are the coordinates of the point on which the load o is applied. The global equilibrium equations allow one to obtain the vertical and horizontal reactions: the vertical reaction at the left support, V_l, the vertical reaction at the right support, V_r, and the horizontal thrust at the right support, H_r.

The position of the points defining the thrust line, P_i and P_{i+1}, and the axial force, N, acting on each of those points are obtained using the vertical forces, horizontal forces and moment equilibrium equations for each voussoir (Fig. 5, left). They can be expressed as follows:

$$V_i = W_{c_i} + W_{tv_i} + VL_i + V_{i+1} \tag{4}$$

$$H_i = Hw_{c_i} + Hw_{tv_i} + HL_i + H_{i+1} \tag{5}$$

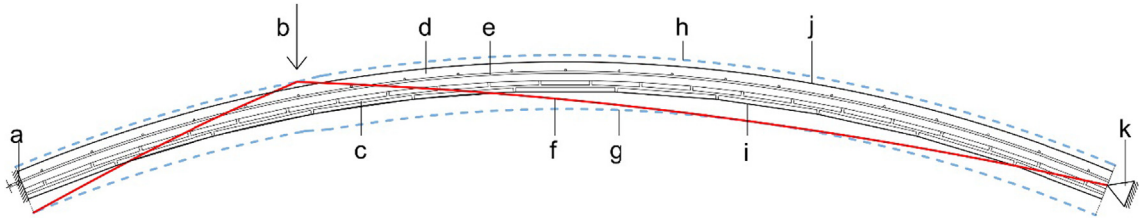

Fig. 4. Application of uniqueness theorem with ELARM: (a) fixed support, (b) applied load, (c) tile vault, (d) concrete, (e) reinforcement, (f) thrust line, (g) lower virtual thickness, (h) upper virtual thickness, (i) real lower thickness, (j) real upper thickness, (k) pinned support.

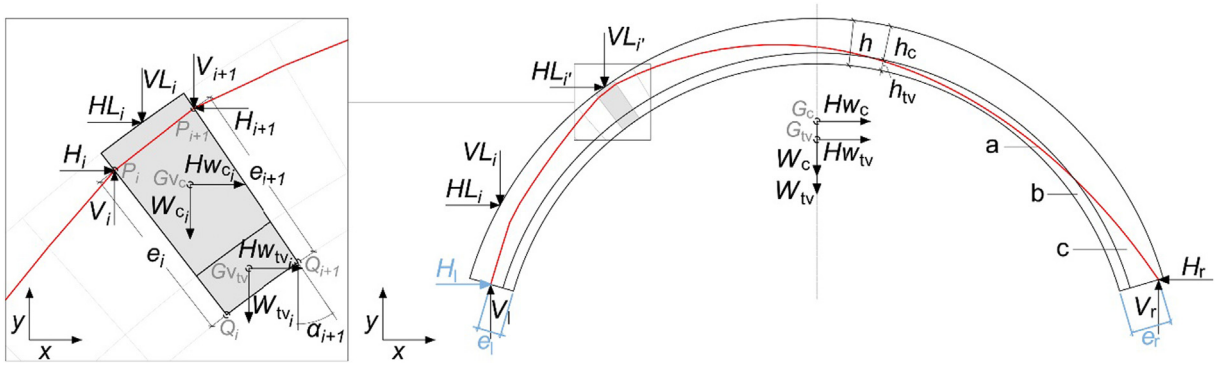

Fig. 5. (Left) Forces acting on each fictitious voussoir. (Right) Global equilibrium, (a) thrust line, (b) tile vault, and (c) concrete.

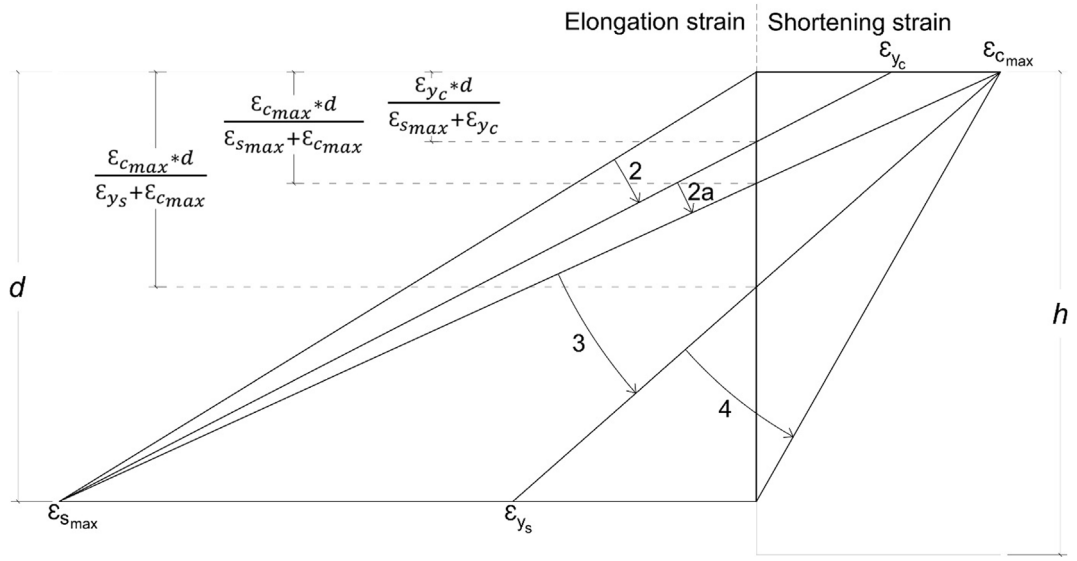

Fig. 6. The different strain domains that the cross-section state can be within.

$$H_i y_{H_i} + HL_i y_{HL_i} + VL_i x_{VL_i} + W_{c_i} x_{W_{c_i}} + Hw_c y_{Hw_c} + W_{tv} x_{W_{tv}} + Hw_{tv} y_{Hw_{tv}} + V_{i+1}(x_{Q_{i+1}} + e_{i+1} sin\alpha_{i+1}) = V_i x_{V_i} + H_{i+1}(y_{Q_{i+1}} + e_{i+1} cos\alpha_{i+1}) \quad (6)$$

where x_k and y_k are either the coordinates of the point k or the coordinates of the point on which the load k is applied and α the angle of the voussoir's joint with a vertical plane (Fig. 5, left). These equations are computed for each voussoir to obtain the vertical and horizontal forces acting on them, V_{i+1} and H_{i+1}, and the distances, e_{i+1}, from the intrados to the position of the points defining the thrust line, P_{i+1} (Fig. 5, left). Knowing V_{i+1} and H_{i+1}, the axial and shear forces, N and S, can be computed for each voussoir using the following equations respectively:

$$N_{i+1} = V_{i+1} sin\alpha_{i+1} + H_{i+1} cos\alpha_{i+1} \quad (7)$$

$$S_{i+1} = V_{i+1} cos\alpha_{i+1} - H_{i+1} sin\alpha_{i+1} \quad (8)$$

The cross-section can be then checked against shear using the equations for reinforced concrete in clause 6.2.2 from Eurocode 2 [23]. The axial force is used during the cross-section analysis to compute the new virtual thickness.

3.6. Cross-section analysis. New virtual thickness

The method adopted for the calculation of the ultimate sectional moments is based on the approach presented in Eurocode 2 for reinforced concrete [23] and Eurocode 6 for reinforced masonry [24] for members subjected to combined axial loading and bending moment. The stress-strain relationship of concrete or masonry are taken to be linear or rectangular depending on the strain state of the materials. The cross-section is analysed in bending at its ultimate limit state, meaning that either the steel, the concrete or the tile vault masonry have reached their ultimate strain, which is set to 0.01 for steel ($\varepsilon_{s_{max}}$) and 0.0035 for concrete ($\varepsilon_{c_{max}}$) or tile vault masonry ($\varepsilon_{tv_{max}}$) according to [23,24].

The masonry's strain and deformation under both its self-weight and the concrete's weight before curing are considered negligible and are not taken into account for the calculation of the ultimate sectional strengths. The local point loads that would be expected during construction, for which the tile vault needs to be dimensioned as well, represent a much more significant loading condition on a compression-only structure than the relatively-low distributed dead weight load of the thin concrete layer. The local point loads become therefore the governing loads determining the thickness of the tile vault. In this context, the resulting strain state in the thin tile layer caused by only its own self-weight and that of the concrete layer, is negligible in comparison with the magnitude of the strain at the ultimate state. This has been checked through a comparison of strains in a finite element model of the tested vaults (Section 5), in which the maximum compressive strain of the tile vault supporting its self-weight and the concrete layer's weight represents 0.39% of the ultimate compressive strain, $\varepsilon_{tv_{max}}$. Furthermore, the maximum deformation of the model (calculated as 0.077 mm) is 0.25% of the tested vaults' maximum deformation at the peak load (29 and 32 mm). Even though the mentioned strain and deformation are considered negligible, further research on this method could involve the modification of the algorithm to include this

deformation in a similar way as it is done in Marmo et al. [25].

According to Fig. 6, the possible strain domains for the cross-section at this ultimate limit state are labelled 2, 2a, 3 and 4. Subdivision 2a in domain 2 is considered depending on whether the concrete or masonry have reached their yield limit. The identification of these selected domains is important, as each indicates a different stress-strain state of the materials and corresponds to a different system of equations to solve for the equilibrium of the cross-section. Domain 2 corresponds to failed steel and non-yielded concrete or masonry, whereas in domain 2a the concrete or masonry have reached their yield stress. Domain 3 corresponds to crushed concrete or masonry and yielded steel, while in domain 4 the steel has not reached its yield stress. The limits of the strain domains are determined by the position of the neutral axis, which is defined here by the distance of the most compressed fibre to the neutral axis (x). From the deformation compatibility equations, the mentioned limits can be expressed as follows:

$$0 \leq x_2 \leq \frac{\varepsilon_{y_c} d}{\varepsilon_{s_{max}} + \varepsilon_{y_c}} \leq x_{2_a} \leq \frac{\varepsilon_{c_{max}} d}{\varepsilon_{s_{max}} + \varepsilon_{c_{max}}} \leq x_3 \leq \frac{\varepsilon_{c_{max}} d}{\varepsilon_{y_s} + \varepsilon_{c_{max}}} \leq x_4 \leq \mathrm{d} \tag{9}$$

where x_n are the values of x in the *n-th* domain, ε_{y_s} is the tensile yield strain of the steel and ε_{y_c} is the assumed compressive yield strain of the concrete and d is the effective depth of the section (i.e., the distance between the most compressed fibre in the section and the centroid of the reinforcement layer).

The assumed distribution of strains, stresses and forces in the cross-section for each strain domain can be seen in Fig. 7. The distance x of the neutral axis to the most compressed fibre at the ultimate limit state in bending for a given axial force, N, can be calculated from the equilibrium equations in each strain domain. A perfectly plastic bi-linear stress-strain relationship is considered for the reinforcement steel, whereas for the masonry and concrete, a linear stress-strain relation is applied in the elastic range and a rectangular stress block distribution in the plastic state [24].

The force experienced by the reinforcement, T_s, is computed using a different equation depending on whether the steel has yielded (domains 2, 2a and 3) or not (domain 4). For the former case, the following expression is used:

$$T_s = A_s f_s \tag{10}$$

where A_s is the total area of the steel reinforcement and f_s is its tensile yield strength.

In the case of an ultimate bending moment leading to the steel stresses in their elastic range, i.e. domain 4, the force T_s results from:

$$T_s = A_s E_s \varepsilon_s \tag{11}$$

with E_s the steel's Young's Modulus and ε_s the current strain level, obtained from the strains' deformation compatibility equations (Fig. 7, green diagrams):

$$\varepsilon_s = \frac{\varepsilon_{k_{max}} (d - x)}{x} \tag{12}$$

where $\varepsilon_{k_{max}}$ is the ultimate strain of the concrete ($\varepsilon_{c_{max}}$) or the tile vault ($\varepsilon_{tv_{max}}$).

The compression, C, experienced by either the concrete or the tile vault (positive or negative moment respectively) on its plastic range, i.e. domains 2a, 3 and 4, is computed considering a rectangular stress block distribution via the following equation [23]:

$$C = 0.8 x b f_k \tag{13}$$

where f_k is the compressive strength of the concrete or tile vault and b is the width of the vault.

For domain 2, where a linear stress-strain relation is applied, the compression force can be written as

$$C = \frac{1}{2} x b E_k \varepsilon_k \tag{14}$$

with E_k the concrete's or tile vault's Young's Modulus and ε_k the maximum compressive outer fibre strain, obtained from the strains' deformation compatibility equations (Fig. 7, green diagrams):

$$\varepsilon_k = \frac{\varepsilon_{s_{max}} x}{d - x} \tag{15}$$

These expressions are related through the horizontal forces equilibrium equation:

$$C = N + T_s \tag{16}$$

from which the distance of the neutral axis to the most compressed fibre at the ultimate limit state can be obtained. For domain 2:

$$x_2 = \frac{-(2N + 2A_s f_s) \pm \sqrt{(2N + 2A_s f_s)^2 - 4(\varepsilon_{s_{max}} E_k b)(-2A_s f_s d - 2Nd)}}{2\varepsilon_{s_{max}} E_k b} \tag{17}$$

For domains 2a and 3:

$$x_{2a,3} = \frac{N + A_s f_s}{0.8 b f_k} \tag{18}$$

For domain 4:

$$x_4 = \frac{-(A_s E_s \varepsilon_{k_{max}} - N) \pm \sqrt{(A_s E_s \varepsilon_{k_{max}} - N)^2 - 4(0.8 b f_k)(-A_s E_s \varepsilon_{k_{max}} d)}}{2 * 0.8 b f_k} \tag{19}$$

The computational implementation allows a scanning of all the different strain-stress states, disregarding the x values that are not within the corresponding domain (Eq. (9)), reducing the possibilities to a unique x and a unique ultimate strain-stress state.

The moment equilibrium equations are then used to calculate the eccentricity e, both for the positive and negative moment, e_p and e_n (Fig. 7), which correspond to the upper and lower virtual thickness limits respectively. Computing the moments from the most compressed fibre, i.e. at the top of the cross-section in the case of the positive moments and at the bottom for negative moments, the eccentricity e for domain 2 can be written as

$$e = \frac{T_s d - C\frac{x}{3}}{N} \tag{20}$$

whereas for domains 2a, 3 and 4, it can be written as

$$e = \frac{T_s d - C\frac{0.8x}{2}}{N} \tag{21}$$

4. Computational implementation

The developed tool allows a responsive, intuitive and interactive process of design and structural analysis of composite vaults. The parametrisation of the geometrical inputs, external loads and material properties and quantities, permits the application of the method to different types of reinforced concrete or masonry structures, a user-friendly form-finding process and a straightforward analysis of different geometries, loading combinations and cross-sectional configurations. The flow diagram in Fig. 8 illustrates the process for the design and/or structural analysis with this tool based on the Extended Limit Analysis of Reinforced Masonry. Once the mentioned inputs are introduced, the thrust line and virtual thickness are computed and drawn. If the vault is not stable or the design is not satisfactory, the inputs can be modified either through a size or a shape optimisation process. The size optimisation involves modifying the reinforcement's position or quantities, the materials strength or the thicknesses of the different material layers. The shape optimisation is carried out by modifying the geometry of the structure to be able to contain the thrust line within its virtual

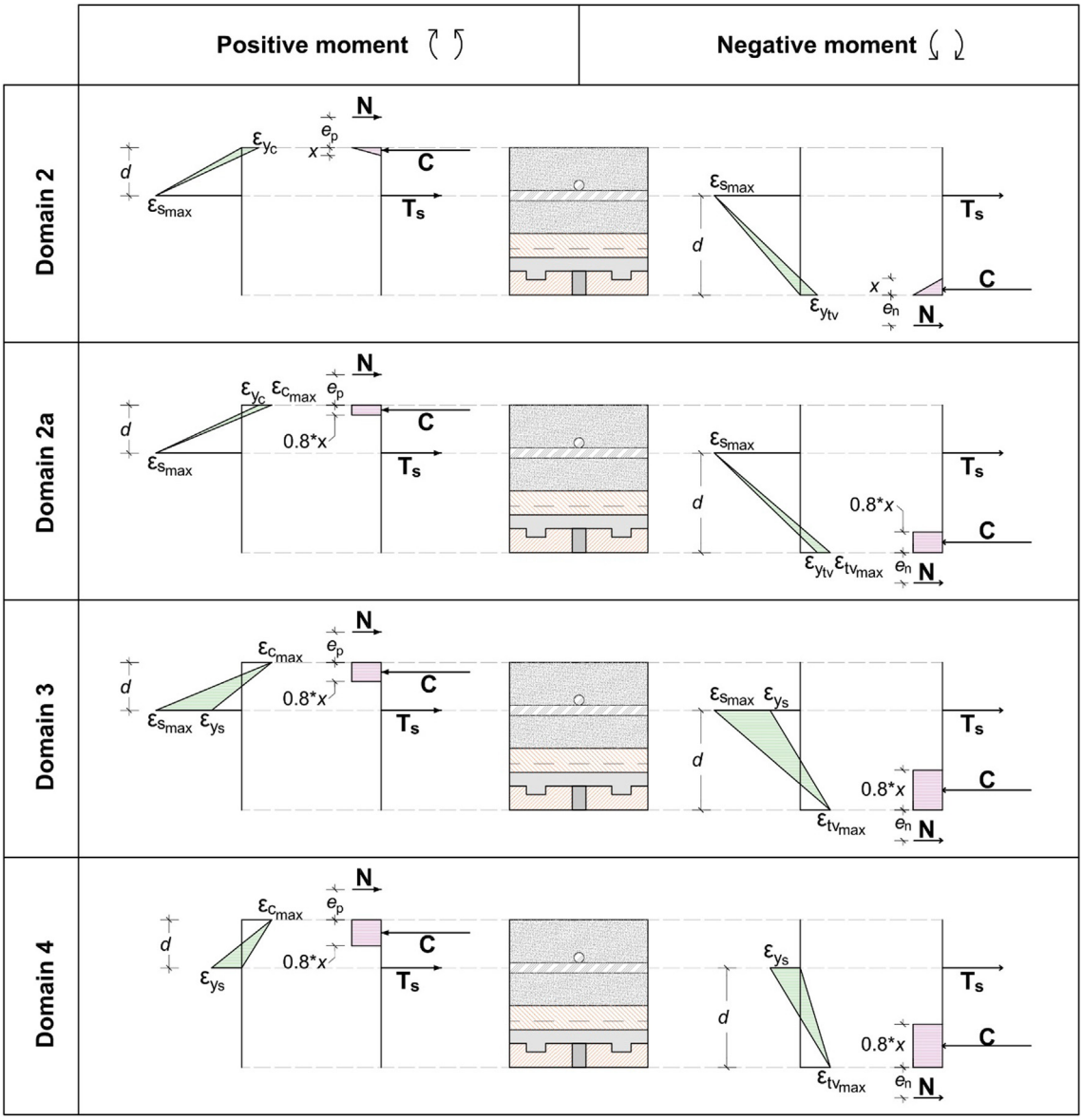

Fig. 7. Distribution of strains, stresses and forces in the different strain domains.

thickness' limits. Both of these structurally informed processes are carried out with the immediate feedback from ELARM, which automatically computes the thrust line and virtual thickness again. Once a stable and satisfying vault is achieved, further load combinations can be checked if needed.

The computational implementation has been coded in the scripting language Python and uses the software Rhinoceros and plugin Grasshopper to visualise the results and to introduce and modify input parameters.

4.1. Safe theorem

According to the safe theorem, "*If a line of thrust can be found which is in equilibrium with the external loads and which lies wholly within the masonry, then the structure is safe.*" [14]. Note, that in this case, we look for a thrust line staying within the new virtual thickness.

Every thrust line results from the combination of the values of the three variables H_l, e_l and e_r. These parameters are varied and combined according to ranges and divided by small increments as defined by the user, in order to scan (in a discrete manner) all the possible thrust lines of the structure. Any of the thrust lines lying entirely within the virtual thickness satisfy the safe theorem. However, a single thrust line is chosen to be drawn and to determine the value of the three parameters. For each point defining a thrust line, the distances to the upper limit, d_{u_i}, and to the lower limit, d_{l_i}, of the virtual thickness are measured, squared and summed. A summation of each point's resulting values is computed for each thrust line, which has therefore an associated number, R, indicating how far the thrust line is, on average, from the limits of the virtual thickness, i.e., how central its position is in relation to those limits. This can be expressed as follows:

$$R = \sum_{i=0}^{n} ({d_{u_i}}^2 + {d_{l_i}}^2) \tag{22}$$

where n is the number of fictitious voussoirs and i indicates the specific joint of the fictitious voussoir on which the distances, d, are computed. The thrust line having the lowest associated value of R is then chosen.

4.2. Uniqueness theorem

According to the uniqueness theorem, *"If a line of thrust can be found which represents an equilibrium state for the structure under the action of the given external loads […] and which allows the formation of sufficient hinges*

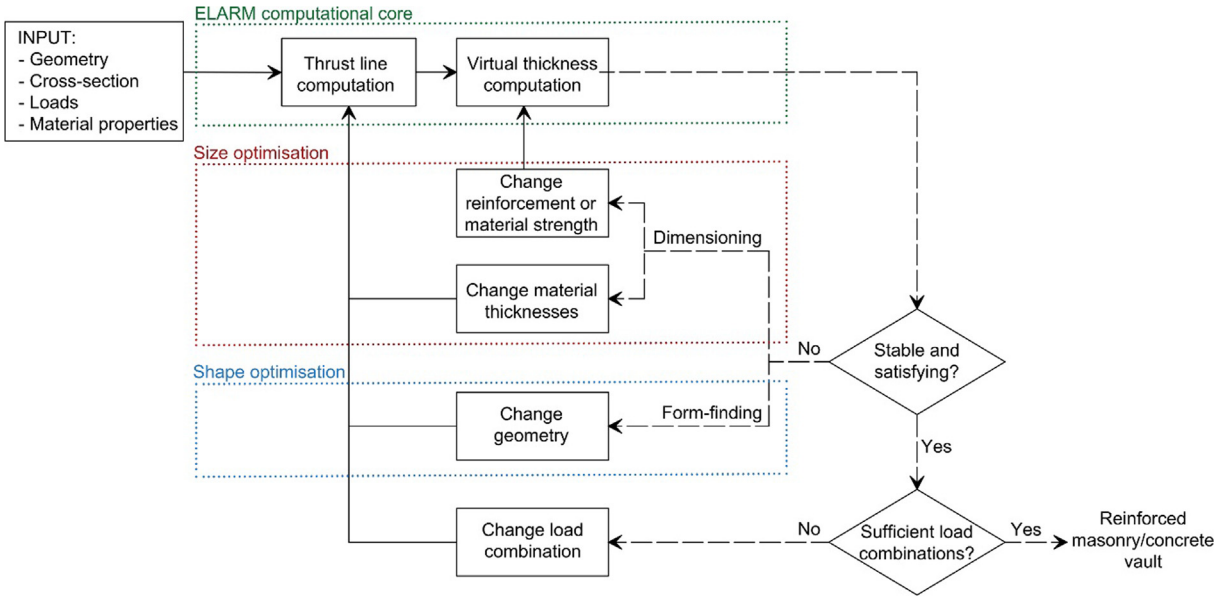

Fig. 8. Flow diagram of the computational approach.

to transform the structure into a mechanism, then the structure is on the point of collapse" [14].

The uniqueness theorem is computationally implemented by applying an incremental factor to the external loads, scanning the possible thrust lines and selecting the one creating the mechanism. For a given load condition, small increments of the multiplier factor are applied to the external loads. The possible thrust lines of the structure, resulting from the combination of the three variables H_l, e_l and e_r according to certain domains and increments defined by the user, are checked for every incremented load condition. Among all the resulting thrust lines lying entirely within the virtual thickness bounds, the selected solution is the one with the highest load multiplier factor. This solution is the only one tangent to the virtual thickness' limits in the sufficient number of alternating intrados-versus-extrados points as to create the hinges required to transform the structure into a mechanism.

5. Load tests on full-scale prototypes

In order to validate both the construction technology and the proposed computational implementation, a set of experiments was carried out at the Laboratory for Technological Innovation in Structures and Materials (LITEM) at the Polytechnic University of Catalonia (UPC).

Two full-scale prototypes were built and load-tested to failure. The vaults were cylindrical in shape and had a span of 2.78 m, a height of 0.25 m and a width of 1 m. The two vaults were composed of a two-layered, 36-mm-thick tile vault and a 50-mm-thick reinforced concrete layer (Fig. 9). The tiles had sizes of 277 × 134 × 13 mm. The first course ones had a smooth side facing the intrados and 6.5-mm-deep grooves to receive the mortar, whereas the ones at the second course included a rough, striped, top face to increase the contact with the concrete instead of the smooth surface (Fig. 2). The binders were fast-setting cement for the first course of tiles and Portland cement mortar for the second one and the 10-mm joint in between courses. The reinforcement, placed at the central level of the concrete layer, consisted of 6-mm-diameter steel rebars at 7 cm spacings in both directions (Fig. 10). The boundary conditions consisted of pinned supports that were able to rotate, but translationally constrained (Fig. 11). These hinges at the supports were blocked (not allowed to rotate) during construction, so that the barrel vaults could have been built in the traditional way, i.e. without the need of a formwork, except at one of its boundaries (only required for the first row of bricks to form the first arch/stable section). However, seeking the maximum possible accuracy

Fig. 9. Photo of one of the full-scale prototypes. View of the intrados showing the tile vault's pattern.

in the construction of these laboratory specimens, the vaults were built using a complete formwork.

A vertical load was applied at quarter span to a loading pad with a breath of 115 mm and stretching the entire width of the vault. The test was carried out under displacement control at a constant speed of 0.4 mm/min until failure.

Fig. 12 shows the load-displacement curves of the two tested vaults. Both vaults developed the same mechanism with the formation of two hinges (the supports were pinned). The first hinge was located under the loading platform and the second one, at the opposite side of the vault, revealed itself not as a single crack, but as a group of cracks on the extrados due to the reinforcement's influence (Fig. 13). Composite vault 2 featured a post-peak plastic behaviour and an unloading response up to a displacement of 76 mm, beyond which no further load could be applied due to the delamination between masonry and concrete. The peak load was 53.15 kN.

In vault 1, the test stopped before the expected unloading branch due to debonding as well. Considering the match of the two plots at the first stretch in Fig. 12, the observed cracks at the extrados of the vaults evidencing the formation of the second hinge (Fig. 13) and the almost null stiffness reached around the peak load (note the slopes'

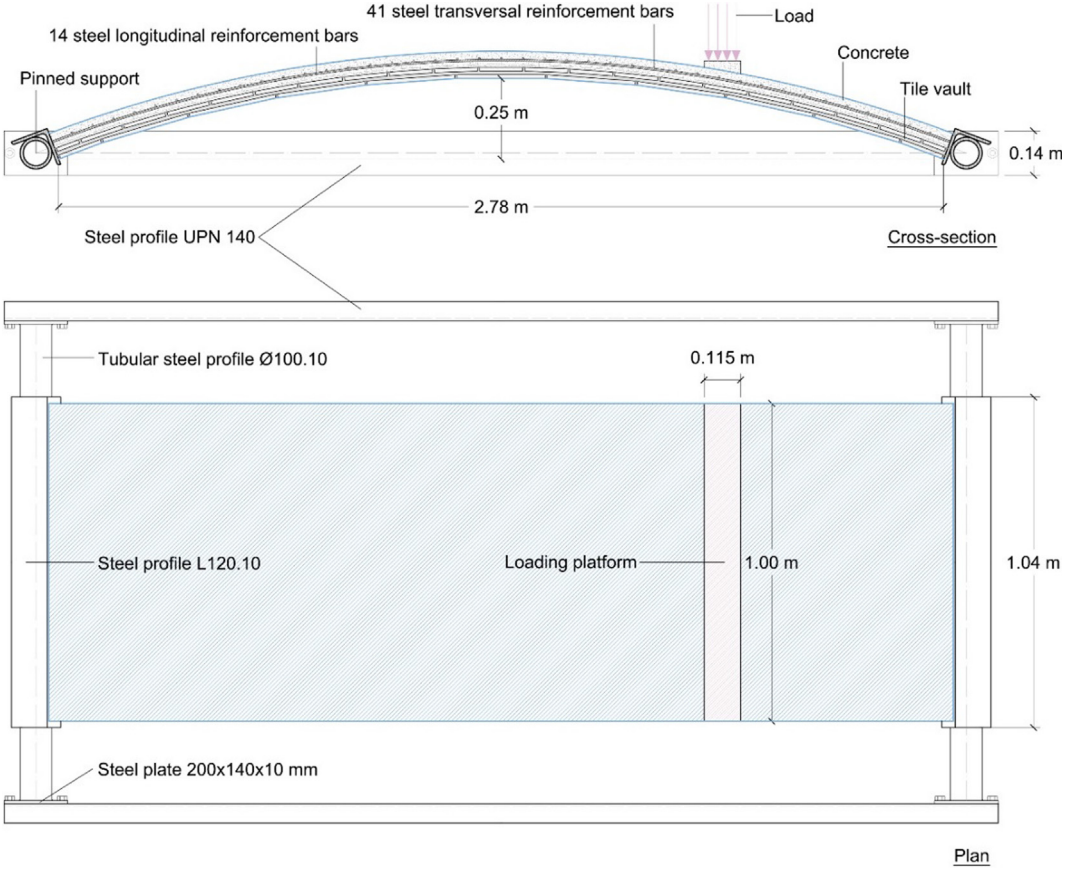

Fig. 10. Setup of the prototype for the load test. (Top) cross-section, (Bottom) plan view.

Fig. 11. Detail of the pinned support.

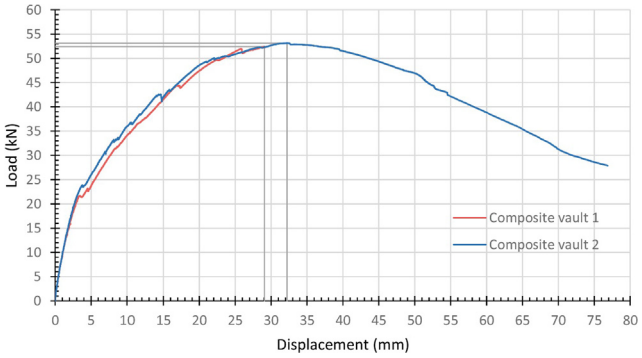

Fig. 12. Ultimate load test. Load-displacement curves of the two composite vaults.

horizontality of the load-displacement curves), the authors conclude that debonding occurred either simultaneously or right after the generation of the second hinge, linked to the excessive deformation due to the formation of the mechanism. This fact prevented the development of the expected post-peak unloading branch. The load-displacement curve showed a non-linear behaviour until failure with an ultimate load of 52.43 kN for a vertical displacement of 29 mm at the loading point.

From these results, the system showed in principle the ductility required for the use of limit analysis for its assessment. However, sufficient shear bond at the interfaces between all layers of the designed composite cross-section has to be guaranteed. In order to grant sufficient ductility, an improvement of the shear bond strength could be attained by using masonry units with deeper grooves in contact with the concrete for mechanical keying action, or by integrating shear connectors in the cross-section, such as steel shear studs or nails.

6. Material characterisation

The characterisation of the tile vault presents various difficulties due to its heterogeneity, slenderness, handmade fabrication and multilayer condition. Its compressive strength was estimated from the properties of the material components (tiles, Portland cement mortar and fast-setting cement). Considering the orthotropic behaviour of the tiles, they were tested in the longitudinal and in the transversal directions, which coincide with the alignment of the loads in relation to the bricks in the first and the second course of the tile vault respectively (Fig. 2). Four compression tests were carried out for each case. The mean value for the bricks with the load applied in the longitudinal direction (load applied as in the first course of the tile vault) was 111 N/

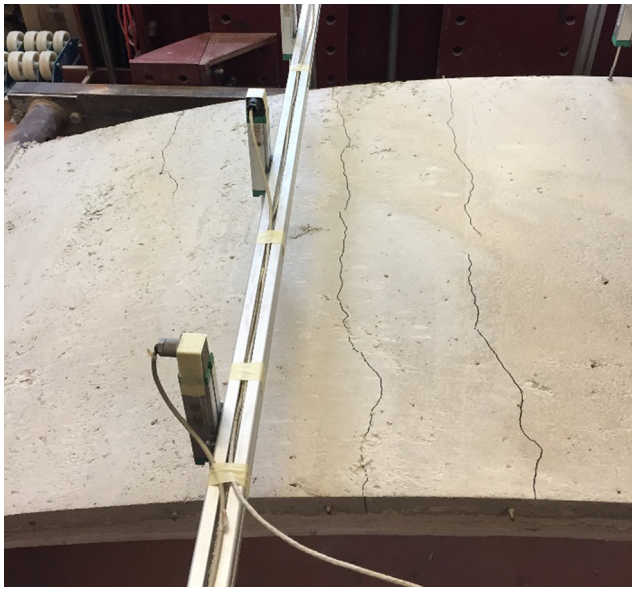

Fig. 13. Cracks on the extrados evidencing the development of the second hinge at the composite vault 1.

mm^2, whereas for the bricks with the load applied in the orthogonal direction (load applied as in the second course of the tile vault) the result was 87 N/mm^2. Portland cement mortar and fast-setting cement were tested in compression with average results for the compressive strength of 6.98 N/mm^2 and 4.47 N/mm^2 respectively. Nine masonry samples were weighed, resulting in an average unit weight of 2000 kg/m^3.

A curved (faceted) structure built with straight masonry units features unavoidably slight variations of its thickness. The construction of the first course of the tested vaults maintained the centre of the tiles tangent to a fictitious cylindrical intrados. Due to this fact and for the presented vault's geometry and tile's sizes, the tile vault had a maximum thickness of 36 mm, which decreased 2.4 mm at the intrados' transversal joints. The tile vault's thickness is therefore taken as the resulting 33.6 mm.

Eurocode 6 [24] offers an equation for the estimation of the masonry's compressive strength,

$$f_k = K f_b^{0.7} f_m^{0.3} \tag{23}$$

where f_k is the characteristic compressive strength of the tile vault in N/mm^2, K is a constant, f_b is the normalised mean compressive strength of the units (to be taken not greater than 75 N/mm^2 in the direction of the applied action effect), and f_m is the compressive strength of the mortar, also in N/mm^2.

The tile vault's entire cross-section cannot be clearly classified within the Eurocode 6, mainly due to its multilayer condition and its continuous thick mortar joint parallel to the intrados and extrados (Fig. 2). Therefore, the compressive strength of each of its three layers (first course of bricks, mortar layer and second course of bricks) has been considered separately to compute subsequently a total compressive strength of the tile vault taking into account the thickness of each layer. The tiles are considered solid and the thicknesses of the two courses of tiles are taken as the tile's total thickness subtracting the grooves' depth (6.5 mm). The considered thickness of the in-between mortar layer is increased adding the grooves' depth of both the upper and lower tiles. Therefore, the three layers consist of: (1) 6.5-mm-thick masonry composed of tiles in the longitudinal direction with fast-setting cement joints, (2) a 20.6-mm-thick mortar joint, and (3) 6.5-mm-thick masonry composed of tiles in the transversal direction with Portland cement mortar. The compressive strength of (2) is the one of the mortar (6.98 N/mm^2), whereas Eq. (23) is used for (1) and (3). Constant K is determined from Table 3.3 from Eurocode 6, in which the material and group of the masonry units, together with the kind of mortar have to be introduced. For clay masonry units classified in group 1 and general purpose mortar, Table 3.3 provides a value of K equal to 0.55. The tests of the different materials composing the tile vault allow obtaining f_b and f_m. The results from the compression tests on tiles in both directions were over 75 N/mm^2, which is therefore the value taken as f_b in Eq. (23) for both (1) and (3). For the first course, joined with fast-setting cement, f_m is taken as 4.47 N/mm^2, whereas for the second course of tiles, joined with Portland cement mortar, f_m is taken as 6.98 N/mm^2. With these values, Eq. (23) provides the characteristic compressive strength, which is divided by 0.8 to obtain the average compressive strength [26]. The entire tile vault's compressive strength is estimated by multiplying each strength by the corresponding thickness, summing the results and dividing by the total thickness of the tile vault, with a result of 13.45 N/mm^2.

Ten 100-mm cubic samples of concrete were produced during the construction of the two prototypes. The results of the compression tests gave a mean value $f_{c,cube}$ equal to 27.75 N/mm^2. A factor of 0.8 was used to convert the average compressive strength of cubic samples to a 150-mm-diameter by 300-mm-high cylindrical samples (as documented in Eurocode 2 [23]). The result is a concrete compressive strength of f_c equal to 22.20 N/mm^2, which is the value used in the model. The unit weight of the concrete was calculated as 2460 kg/m^3.

Ten 6-mm-diameter steel reinforcement bars were tested in tension to obtain their yield tensile strength and Young's modulus. The mean yield tensile strength was equal to 581 N/mm^2 and the Young's Modulus was equal to 207,000 N/mm^2.

7. Comparison of results.

The geometry of the vaults and the material properties indicated in the previous section were introduced into the computational model to apply the uniqueness theorem and obtain the ultimate load carrying capacity of the vault (Fig. 14). The thrust line's ends were set to the cross-section's centre line to represent the pinned support condition (Fig. 11). The vault was divided into 100 voussoirs and the load was applied evenly as point loads onto four voussoirs at quarter span, replicating the 11.5-cm-wide loading platform of the experimental tests.

The load predicted by the numerical method is 53.6 kN (Fig. 14), which is 1.5% higher than the average of the two values obtained in the experimental tests, 52.8 kN. The results of the cross-sectional analysis with ELARM showed that the failure had occurred with concrete at its ultimate strain and steel not yielded for the positive moment and tile vault at ultimate strain and steel yielded for the negative moment. The position of the neutral axis in the case of the negative moment (between 32.1 and 32.8 mm from the intrados) showed the compression stress block as fully developed within the tile vault (33.6 mm thick).

In addition to the uncertainty in the compressive strength of the masonry layers (for which only an estimation is available as described

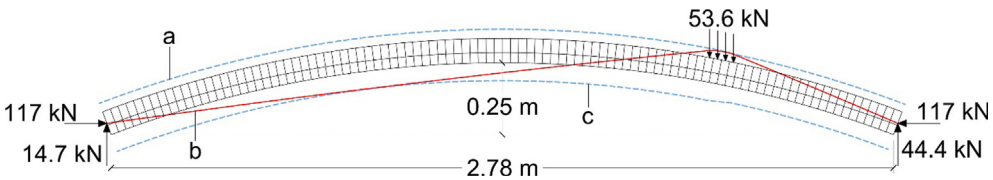

Fig. 14. Application of the uniqueness theorem with ELARM to the tested vaults: (a) upper virtual thickness, (b) thrust line, and (c) lower virtual thickness.

in Section 6), small deviations in the prediction of the ultimate load can be explained by the handmade condition of the structure, in which, even with an exhaustive construction control, small fluctuations on the mortar and cement strength are expected and little variations on the thicknesses may occur frequently.

It is important to highlight that even though the cross-section introduced in ELARM does not vary along the length of the vault, the computed virtual thickness, as well as the position of the neutral axis and the equilibrium of forces in each voussoir are different because of the changing axial force, *N*, which varies according to the external forces and the self-weight of the structure. An external load increases the axial force, which reduces the eccentricity for the same resisted bending moment. This is the reason why the virtual thickness experiences a sudden narrowing where the loads are applied.

8. Form-finding and optimisation procedures

The ELARM implementation coded in Python, results in an interactive tool providing quick structural feedback. As can be expected from any computational implementation, it offers speed, accuracy and the possibility to extend the analysis to similar structures with different sizes or properties. The next subsections describe specific features that this method offers for the design and structural analysis of reinforced masonry/concrete arches.

The use of the software Rhinoceros and the plug-in Grasshopper for the visualisation of graphical results and for the efficient introduction and modification of input parameters, allows for a fast and user-interactive form-finding process. The starting intrados of the analysed vault can be drawn as a curve in Rhinoceros, which can be easily modified through its control points. As the curve is being adjusted, calculations are computed and graphical updates are provided. The shape and parameters of the vault can be adapted and optimised according to the structural feedback received in near real-time.

8.1. Form finding

The presented tool allows the optimization of the vault's shape regarding a defined loading condition, e.g. the permanent loads acting on the structure, by modifying the inputs that define the vault's geometry, and then adapting to the tool's structural feedback. A shape optimized for certain given loads would be one that includes within its virtual thickness boundaries the thrust line supplied by ELARM with a minimum thickness and reinforcement. Therefore, instead of starting from an invariable, predefined shape and modifying thickness, material strength and/or reinforcement to increase the virtual boundaries and make the thrust line fit within, a form finding process consists of modifying the geometrical inputs of the structure to make geometry and thrust line match as much as other design constraints would allow.

The case study of Gaudí's graphical design for the Laundry Room Portico in Park Güell (Barcelona) is presented as an example of the implementation's interactive feature (Fig. 15). The portico is a covered space featuring inclined columns at one side and a long, curved retaining wall at the opposite side to counteract the soil's thrust (Fig. 15, right). A structure with a traditional arch geometry such as a parabola would be excessively massive given the specific existing loads, which demand a clever structural design to create an efficient structure. Designing the structure with these permanent, asymmetric and predominant dead loads as main inputs is a clever strategy to obtain an approximate efficient solution.

The modification of the vault's shape during the form-finding process should be combined with an iterative process of variation of the vertical and horizontal loads, as they are dependent on the soil's weight and thrust. These loads could be obtained using an algorithm to compute the soil's volume on top and next to the vault each time the intrados is modified. However, to simplify calculations in this example, the vertical and horizontal loads applied are taken as constant throughout the form-finding process. The loads' values decrease gradually as they are applied in a higher position and range from 3 kN to 0.15 kN for the horizontal loads and from 0.9 kN to 0.4 kN for the vertical ones.

The form-finding process for this case study starts by introducing in the model the mentioned constant, predominant and permanent loads (Fig. 15, left, a). The material properties are introduced as well. In this case, it is considered as a masonry structure with a compressive strength of 15 N/mm^2 and a unit weight of 2000 kg/m^3. A curve with a height of 3.75 m (Fig. 15, left, b) is drawn as the input intrados of a preliminary vault and the tool provides immediate structural feedback. Then a process of adjustment of the thrust line and the vault's shape starts by finding a solution in which the thrust line lies entirely in the vault's thickness. The three variables H_l, e_l and e_r and the intrados curve's control points allow the modification of the thrust line and the vault's shape respectively. Once a stable unreinforced masonry vault is found (Fig. 15, left, c), the thickness of the masonry and the steel reinforcement position and amount can be updated considering other loading combinations, including further asymmetric live loads or if a higher safety factor is desired. Fig. 16 shows two examples of this case study's analysis with ELARM, adding at the top of the structure a 2-kN-punctual load (Fig. 16, left) or a distributed 3-kN load (Fig. 16, right). In both cases, reinforcement is needed and placed at a central level of the cross-section (Fig. 16, b). For the former, a reinforcement of 5-mm-diameter steel rebars at 33 cm spacings (equivalent to 59 mm^2/m) is enough, whereas for the latter the same rebars at 16 cm spacings are needed (118 mm^2/m). The steel's yield tensile strength for the reinforcement is taken as 500 N/mm^2.

8.2. Reinforcement optimisation

A cross-section optimisation can be carried-out by adjusting the thickness of the structural layers and the amount and positions of the reinforcement, while accounting for different load combinations. The method permits the placement of the required reinforcement in specific regions along the vault's length. This feature can be very helpful, for example, to check the adequacy of a particular reinforcement scheme in a certain part of the vault, either for design or in the retrofitting of existing structures.

Fig. 17 and Fig. 18 show an example of a specific case with variable distribution of reinforcement. The studied structure is a 3-m-span, 0.5-m-rise, 1-m-wide and 9-cm-thick masonry barrel vault, to which a new permanent load of 7 kN needs to be added due to a hypothetical change in the use of the building. The load is divided into 10 equal loads of 0.7 kN applied on 10 voussoirs at the right-hand-side quarter-span location over a horizontal distance of 0.28 m. The compressive strength of the masonry is taken as 8 N/mm^2 with a density of 2200 kg/m^3, and the steel's yield tensile strength for the reinforcement as 500 N/mm^2.

The possibility to modify the thrust line and the amount and position of the reinforcement, both along the length of the vault and the thickness of the cross-section, allows the exploration of a large range of possibilities for the reinforcement of the existing vault. In this case, the reinforcement is applied at either the extrados (Fig. 17) or the intrados (Fig. 18). The application of reinforcement on the extrados increases the ultimate negative bending moment and affects the lower virtual thickness limit (Fig. 17), whereas the reinforcement on the intrados increases the upper limit (Fig. 18). A small amount of reinforcement equivalent to a steel area of 21 mm^2 and 23 mm^2 was sufficient to obtain a solution applying the uniqueness theorem for the extrados-reinforced and intrados-reinforced vaults respectively. The case with reinforcement partially applied to the extrados results in a larger horizontal thrust because of the shallower thrust line.

8.3. Seismic analysis

A simple preliminary seismic analysis can be carried out by

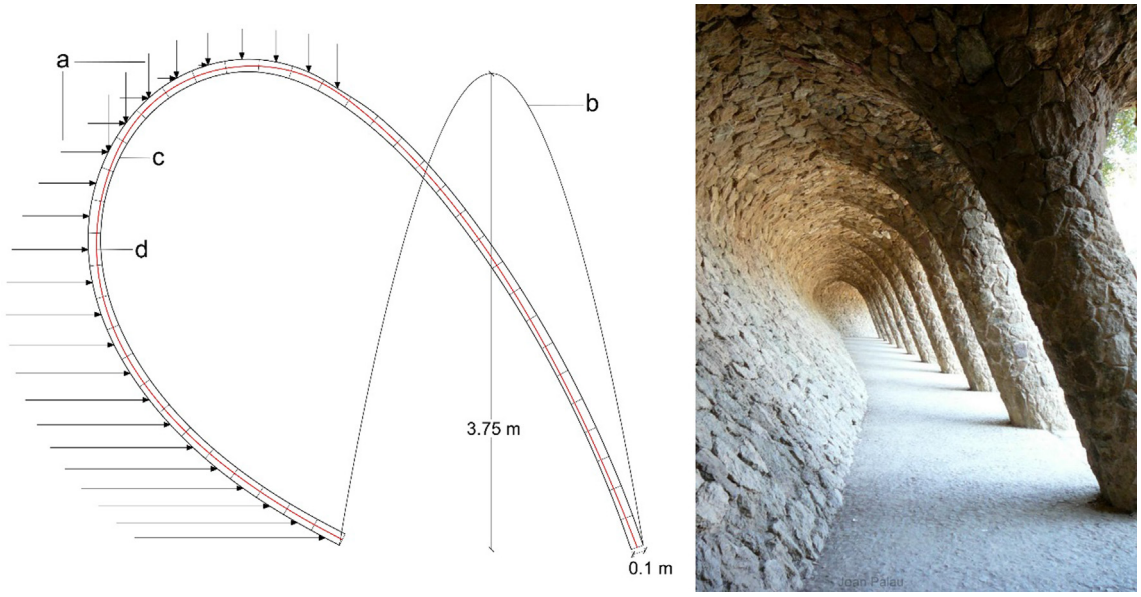

Fig. 15. Case study of Gaudí's graphical design for the Laundry Room Portico in Park Güell (Barcelona). Left) form-finding with ELARM: (a) permanent vertical and horizontal loads, (b) input intrados, (c) form-found shape, and (d) thrust line. Right) view of the Laundry Room Portico.

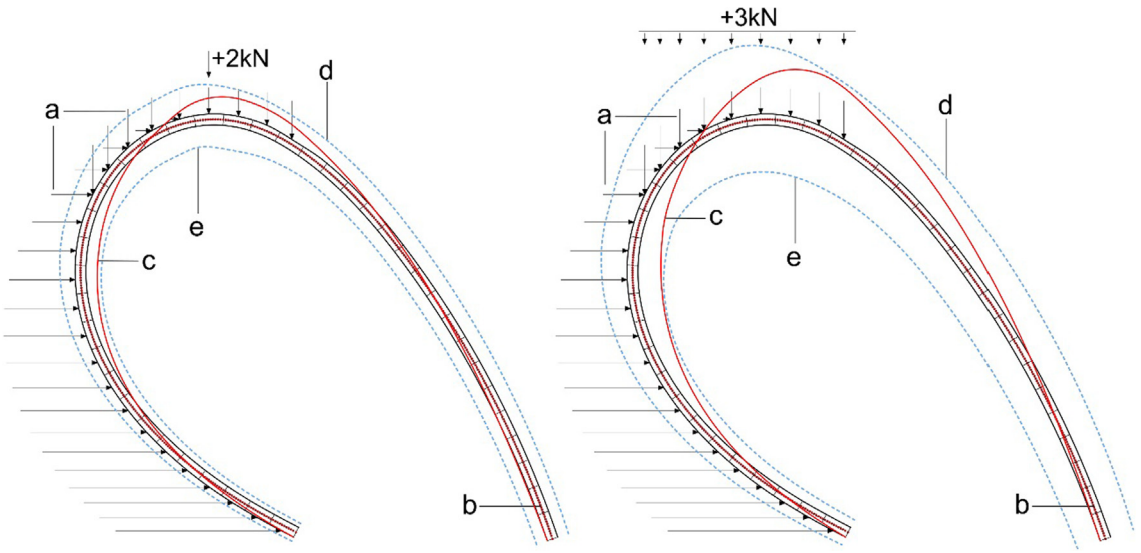

Fig. 16. Examples of loading combinations. (Left) permanent vertical and horizontal loads and a 2 kN punctual load. (Right) permanent vertical and horizontal loads and a load of 3 kN distributed on the top voussoirs. (a) Permanent vertical and horizontal loads, (b) position of the reinforcement, (c) thrust line, (d) upper virtual thickness, and (e) lower virtual thickness.

considering equivalent-static horizontal loads proportional to the vertical self-weight loads. A horizontal load can be applied at the centroids of every voussoir (at both the centroids of the tile vault and concrete portions), equal to its self-weight multiplied by a factor that can be interactively modified by the user, and depends on expected ground accelerations. Fig. 19 shows an example of seismic analysis combining vertical and horizontal loads. The dimensioning of the thickness and reinforcement can be performed as an envelope of different load combinations.

The studied barrel vault is made of a cylindrical composite structure

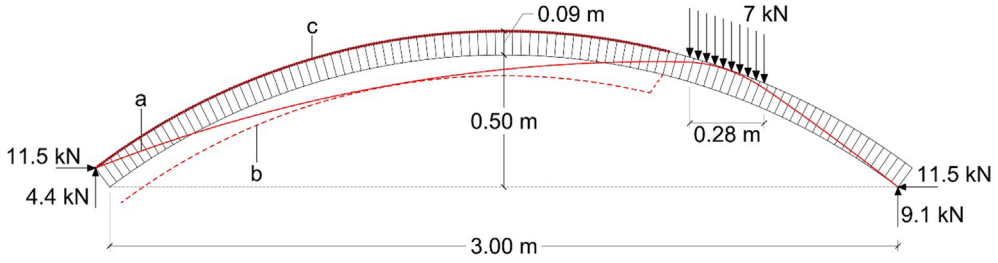

Fig. 17. Partial reinforcement along the extrados of a masonry vault: (a) thrust line, (b) virtual thickness limit, and (c) reinforcement.

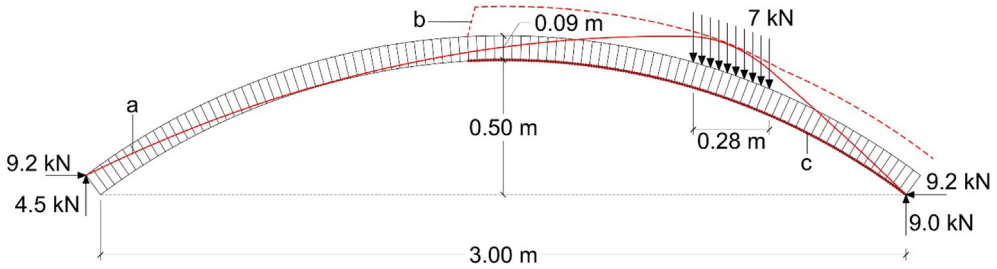

Fig. 18. Partial reinforcement along the intrados of a masonry vault: (a) thrust line, (b) virtual thickness limit, and (c) reinforcement.

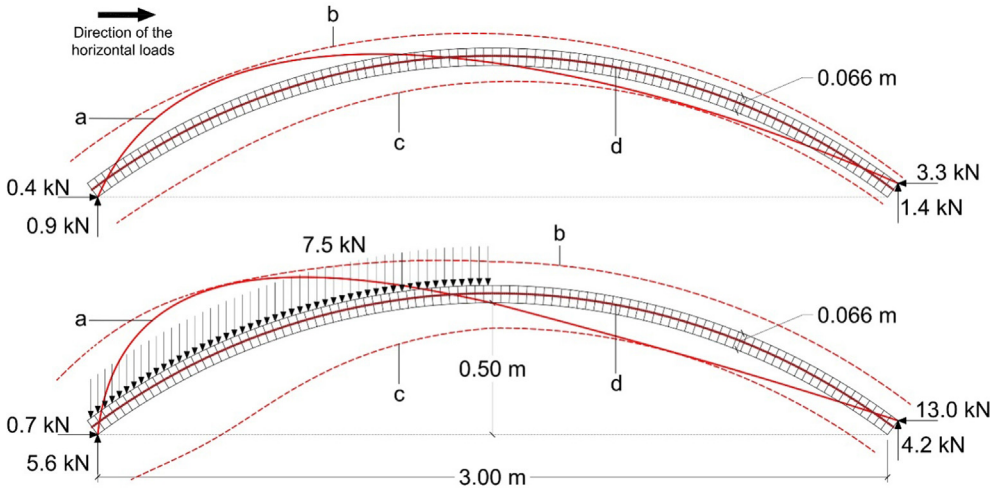

Fig. 19. Seismic analysis with multiplying factor 1.25. (Up) self-weight and horizontal loads. (Down) self-weight, horizontal loads and a load of 7.5 kN. (a) thrust line, (b) upper virtual thickness, (c) lower virtual thickness, and (d) reinforcement.

including a 36-mm-thick tile vault and a thin concrete layer with a thickness of 30 mm. The compressive strength of the tile vault and the concrete are taken as 10 N/mm^2 and 25 N/mm^2 respectively, with densities of 2000 kg/m^3 for the tile vault and 2400 kg/m^3 for the concrete. The steel's yield tensile strength for the reinforcement is 500 N/mm^2. The structure has a span of 3 m and a rise and width of 0.5 m. The supports consist of a contact surface, unable to take bending moments. The horizontal loads are applied in the positive x direction (Fig. 19). For this example, the factor multiplying the self-weight of the vault is taken equal to 1.25. The reinforcement is placed on top of the masonry, at the interface of the tile vault and the concrete. A structural analysis is carried out for two different loading combinations. The first combination includes self-weight and horizontal loads (Fig. 19, up). The second case has an additional vertical load of 7.5 kN (together with its related seismic horizontal load) divided in 50 equal loads of 0.15 kN applied on the 50 voussoirs at the left-hand half-side of the vault (Fig. 19, down). The first case needs very little tensile capacity to remain stable against the applied horizontal loads. The steel reinforcement area was gradually increased until the safe theorem could be fulfilled, reaching only a steel area of 7 mm^2. As expected, the combination adding the 7.5-kN load is more unfavourable, requiring four 5-mm-diameter steel reinforcement bars (total steel area of 78 mm^2).

Additional factors multiplying the self-weight of the structure and converted to horizontal loads have been applied to the same vault, namely, 0.5 (Fig. 20, up) and 1 (Fig. 20, down). Two strategies have been followed to obtain a stable structure: increasing either the reinforcement or the concrete layer's thickness. The unreinforced vault is stable without any change in its thickness considering the multiplying factor 0.5 (Fig. 20, up). The application of horizontal loads corresponding to factor 1 requires a small tensile capacity, achieved with a reinforcement equivalent to a steel area of 4 mm^2 (Fig. 20, down). For this load condition, to remain unreinforced, the thickness of the concrete layer should be increased 40 mm, resulting in a vault's total thickness of 106 mm (Fig. 21, up). For the multiplying factor 1.25, a stable unreinforced vault would have a concrete thickness of 95 mm (an increase of 65 mm and a total thickness of 131 mm), while, as mentioned above, the required reinforcement would only be 7 mm^2 of steel area (Fig. 19, up). The 106-mm-thick vault with a multiplying factor of 1.25, would require a small tensile capacity, equivalent to 3 mm^2 of steel area (Fig. 21, down).

In this case and according to these results, when dealing with seismic loads, the addition of reinforcement provides better results than increasing the mass of the structure.

8.4. Beyond compression-only

The addition of reinforcement to the composite vault allows for the design of structures that are not restricted to being compression-only. These structures, while adding a higher degree of flexibility, versatility and expressivity to the technique, require the use of a formwork to build the non-compression-only parts. Fig. 22, Fig. 23 and Fig. 24 show three examples of different reinforcement and thrust line configurations in a free-form composite vault with a tile vault thickness of 36 mm and a concrete layer of 50 mm. The vault has no external forces applied and has a span of 6 m, a width of 1 m and a rise of 0.75 m at mid-span. The material properties in terms of strength and density are the same as in the previous example in Section 8.3. As ELARM showed ultimate positive bending moments in domain 1 for the examples in Fig. 22 and Fig. 24, the concrete's Young's Modulus is also required for the computation of the virtual thickness and is taken as 27,000 N/mm^2.

The vault features a shape that requires some tensile capacity to be structurally stable. Reinforcement is required in the regions where the thrust line is not contained within the section of the vault. Three different thrust lines are chosen, which result in three different

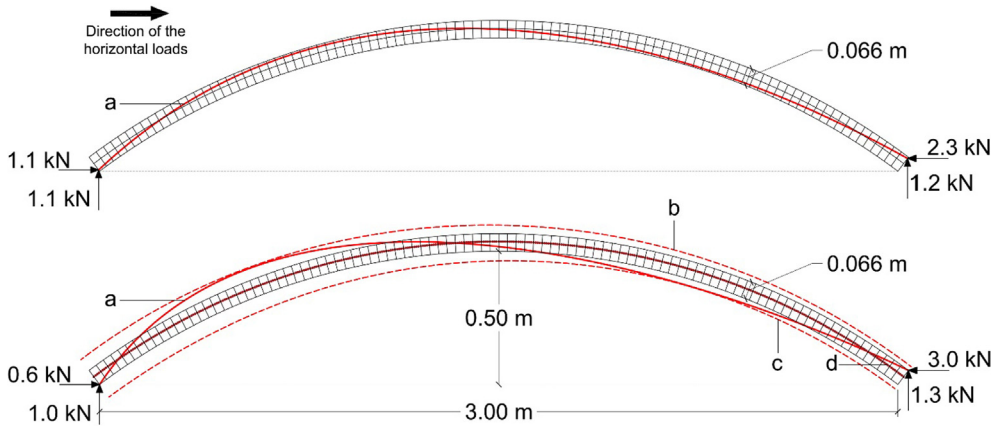

Fig. 20. Seismic analysis: self-weight and horizontal loads. (Up) multiplying factor 0.5. (Down) multiplying factor 1. (a) thrust line, (b) upper virtual thickness, (c) lower virtual thickness, and (d) reinforcement.

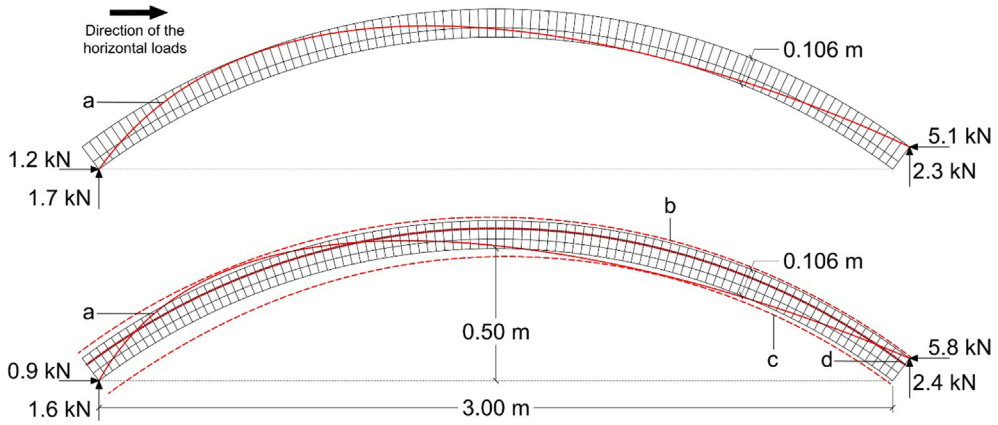

Fig. 21. Seismic analysis: self-weight and horizontal loads. (Up) multiplying factor 1. (Down) multiplying factor 1.25. (a) thrust line, (b) upper virtual thickness, (c) lower virtual thickness, and (d) reinforcement.

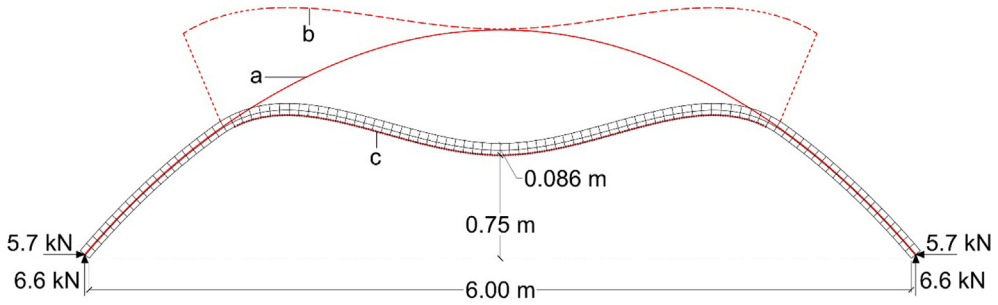

Fig. 22. Free-form composite vault partially reinforced at the intrados: (a) thrust line, (b) upper virtual thickness and (c) reinforcement at the intrados.

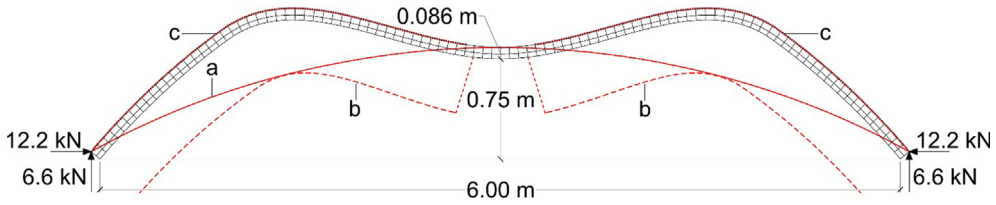

Fig. 23. Free-form composite vault partially reinforced at the extrados: (a) thrust line, (b) lower virtual thickness and (c) reinforcement at the extrados.

reinforcement configurations.

The thrust line in Fig. 22(a) avoids reinforcement in parts of the vault by following the middle line of the cross-section at the first and last 20 voussoirs. In the central part of the vault, due to its shape, the thrust line largely exceeds the physical upper boundary. Therefore, bottom level reinforcement has to be supplied to virtually extend the thickness of the vault upwards (Fig. 22b). The reinforcement is placed at the intrados to maximise the vault's bending capacity for positive moments (Fig. 22c). A reinforcement equivalent to a total steel area of 115 mm^2 (corresponding to 6 steel reinforcement bars of 5 mm

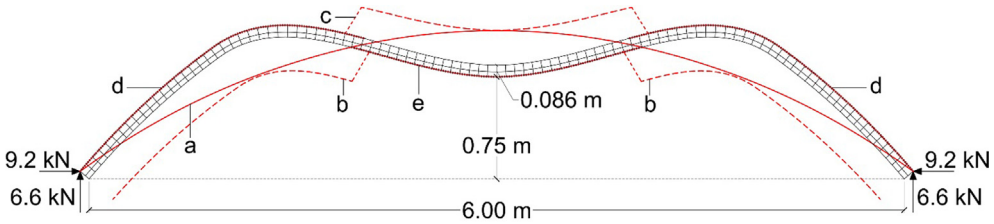

Fig. 24. Free-form composite vault reinforced at both the intrados and the extrados: (a) thrust line, (b) lower virtual thickness, (c) upper virtual thickness, (d) reinforcement at the extrados, and (e) reinforcement at the intrados.

diameter) was introduced in the model and was enough to keep the thrust line within the new virtual boundaries (Fig. 22).

The example in Fig. 23 seeks to avoid reinforcement at the intrados. The thrust line (Fig. 23a) is shallower and the horizontal thrust is thus bigger (12.2 kN against 5.7 kN from the previous example). A total steel area of 136 mm^2 (corresponding to 7 steel reinforcement bars of 5 mm diameter) is applied at the extrados (Fig. 23c). Although in a real construction the reinforcement would very likely be applied on the entire vault's extrados in order to ease the building process and as an additional safety factor, it is worth to highlight that, unlike in the previous thrust line configuration, the central part of the vault would not need any reinforcement, as the thrust line lies within its physical limits (Fig. 23).

The last example (Fig. 24) shows an intermediate solution between the two previous ones. The chosen thrust line (Fig. 24a) has an equal maximum distance from the intrados and from the extrados (when located below or above the vault respectively) and generates also an intermediate horizontal thrust equal to 9.2 kN. The solution requires reinforcement at the intrados of the vault's central part (Fig. 24e) of a total steel area of 57 mm^2 and at the extrados of the remaining parts of the vault for a steel area of 64 mm^2 (Fig. 24d).

The specific steel area multiplied by the length on which it is applied allows the computation of the required volume of reinforcement for each of the three cases, namely 455,400 mm^3, 878,560 mm^3 and 442,980 mm^3 for the examples in Fig. 22, Fig. 23 and Fig. 24 respectively. The solution with the shallower thrust line (Fig. 23) is, in this case, the one requiring more steel. Besides, it is also the option with the highest horizontal thrust. Taking advantage of the vault's funicular shape close to the supports, the thrust line in Fig. 22 reduces the amount of required reinforcement, being only slightly higher than the one required for the most reinforcement-efficient example in Fig. 24, in which the horizontal thrust is, however, 61% higher.

9. Conclusions

A construction technique based on the use of tile vaults as integrated formwork for reinforced concrete has been described. In addition, a 2D method for the design and structural analysis of such composite structures has been presented. The method's computational implementation allows for an interactive and user-friendly form-finding process and a straight-forward assessment with responsive structurally informed feedback. Several examples showing the application to non-compression-only designs, non-uniform reinforcement layouts and horizontal loads have also been discussed.

The construction technique, the method, and the developed computational tool, have been validated through experimental research. Two full-scale prototypes were built and load-tested, allowing the identification of features to improve. In this sense, it is important to consider sufficient bond between the tile vault and the layer of concrete to attain satisfactory structural performance. This can be achieved by using tiles with deeper grooves in contact with the concrete or by integrating shear connectors into the system.

The applicability and accuracy of the proposed analysis method has been validated through its capacity to predict well the results from the experimental results. The method is based on traditional limit analysis, but extends it by considering the tensile capacity of the reinforcement and the compressive strength of the masonry and concrete. The method can also be applied to other structures with a sufficiently ductile response, such as reinforced masonry or concrete arches and vaults, and similar reinforced composite structures combining masonry and concrete.

Acknowledgements

This work was supported by the Swiss National Science Foundation (SNSF), Switzerland [grant number P1EZP2_165203] and the Institute of Technology in Architecture (ITA) at the Swiss Federal Institute of Technology in Zurich (ETH Zurich), Switzerland. It was also sponsored by the construction company URCOTEX, from which Pep Brazo, Antonio Haro and Albert Martí are especially acknowledged. The construction of the prototypes was carried out together with Jordi Domènech, to whom the authors are very thankful.

Experimental support and facilities were kindly offered by the Laboratory for Technological Innovation in Structures and Materials (LITEM) at the Polytechnic University of Catalonia (UPC), from which Lluís Gil, Ernest Bernat, Christian Escrig and Luis Mercedes are especially acknowledged.

References

[1] Huerta S. La mecánica de las bóvedas tabicadas en su contexto histórico: la aportación de los Guastavino. In: Huerta S, editor. Las bóvedas de Guastavino en América. Madrid: Instituto Juan de Herrera; 2001. p. 87–112.
[2] Ramage MH, Ochsendorf J, Rich P, Bellamy J, Block P. Design and construction of the Mapungubwe National Park Interpretive Centre, South Africa. ATDF J (African Technology Development Forum) 2010;7(1/2):14–23.
[3] Block P, DeJong M, Davis L, Ochsendorf J. Tile vaulted systems for low-cost construction in Africa. ATDF J (African Technology Development Forum) 2010;7(1/2):4–13.
[4] Block P, Bayl-Smith M, Schork T, Bellamy J, Pigram D. Ribbed tile vaulting – Innovation through two design-build workshops. In: Gramazio F, Kohler M, Langenberg S, editors. FABRICATE 2014. Zurich: ETH Zurich; 2014. p. 22–9.
[5] Davis L, Rippmann M, Pawlofsky T, Block P. Innovative funicular tile vaulting; a prototype in switzerland. Struct Eng 2012;90(11):46–56.
[6] López López D, Domènech M, Palumbo M. "Brick-topia", the thin-tile vaulted pavilion. Case Stud Struct Eng 2014;2:33–40.
[7] López López D, Domènech M, Palumbo M. Using a construction technique to understand it: thin-tile vaulting. In: Peña F, Chávez M, editors. SAHC2014 – 9th international conference on structural analysis of historical constructions. Mexico City. 2014.
[8] López López D, Van Mele T, Block P. Tile vaulting in the 21st century. Informes de la Construcción 2016;68(544):e162https://doi.org/10.3989/ic.15.169.m15.
[9] López López D, Domènech M. Tile vaults. Structural analysis and experimentation. 2nd Guastavino Biennial. Barcelona: Diputació de Barcelona. 2016.
[10] Truñó A. Construcción de Bóvedas Tabicadas. Manuscript at the Library of the Col·legi d'Arquitectes de Catalunya; ca. 1951.
[11] Tang G. An overview of historical and contemporary concrete shells, their construction and factors in their general disappearance. Int J Space Struct 2015:30(1).
[12] Roca P, López-Almansa F, Miquel J, Hanganu A. Limit analysis of reinforced masonry vaults. Eng Struct 2007;29:431–9.
[13] Kooharian A. Limit analysis of voussoir (segmental) and concrete arches. J Am Concr Instit 1952;49:317–28.
[14] Heyman J. The stone skeleton. Int J Solids Struct 1966;2:249–79.
[15] Heyman J. The masonry arch. Chichester: Ellis Horwood Ltd.; 1982.
[16] Herbert A, Sawyer JR, Kooharian A. Discussion of a paper by Anthony Kooharian: limit analysis of voussoir (segmental) and concrete arches. J Am Concr Instit 1953;25(4). 328-(1–4).
[17] Pippard AJS, Tranter E, Chitty L. The mechanics of the Voussoir Arch. J Inst C.E. 1936;4:281–306.
[18] Pippard AJS, Ashby RJ. An experimental study of the Voussoir Arch. J Inst C.E. 1939;:10.
[19] Pippard AJS, Chitty L. A study of the Voussoir Arch. National Building Studies,

Research Paper No. 11. London: His Majesty's Stationery Office; 1951.
[20] Lourenço PB, Palacio K, Barros J. Design recommendations for reinforced masonry arches. Arch Bridges VI. Barcelona: International Center for Numerical Methods in Engineering (CIMNE). 2004. p. 583–92.
[21] Ramaglia G, Lignola GP, Prota A. Collapse analysis of slender masonry barrel vaults. Eng Struct 2016;117:86–100.
[22] Fabbrocino F, Ramaglia G, Lignola GP, Prota A. Ductility-based incremental analysis of curved masonry structures. Eng Fail Anal 2019;97:653–75. https://doi.org/10.1016/j.engfailanal.2019.01.027.
[23] CEN. Eurocode 2: Design of concrete structures. EN 1992-1-1: 2004. Brussels: CEN; 2004.
[24] CEN. Eurocode 6: Design of masonry structures. EN 1996-1-1: 2005. Brussels: CEN; 2005.
[25] Marmo F, Serpieri R, Rosati L. Ultimate strength analysis of prestressed reinforced concrete sections under axial force and biaxial bending. Comput Struct 2011;89(1–2):91–108. https://doi.org/10.1016/j.compstruc.2010.08.005.
[26] Jäger W, Pech A. Background of the values for compressive strength of masonry acc. to EC6 – evaluation of data. Mauerwerk 2014;18(3–4):229–38. https://doi.org/10.1002/dama.201400629.